CERN-TH/2000-204
BI-TP 2000/22

Finite Temperature Meson Correlation Functions in HTL Approximation

F. Karsch[1,2], M. G. Mustafa[3,4] and M. H. Thoma[2,4a]

[1]Fakultät für Physik, Universität Bielefeld, D-33615 Bielefeld, Germany
[2]Theory Division, CERN, CH-1211 Geneva 23, Switzerland
[3]Theoretical Nuclear Physics Division, Saha Institute of Nuclear Physics, 1/AF Bidhan Nagar, Calcutta - 700 064, India
[4]Institut für Theoretische Physik, Universität Giessen, D-35392 Giessen, Germany

ABSTRACT

We calculate temporal correlators with meson quantum numbers in the deconfined phase of QCD using the hard thermal loop (HTL) approximation. In this way medium effects such as thermal masses and Landau damping in the quark-gluon plasma are taken into account. We show that both effects lead to competing modifications of the free mesonic correlation functions. We find that correlators in scalar channels are only moderately influenced by the HTL medium effects, while the HTL-vertex corrections lead to divergent vector correlators.

[a]Heisenberg fellow

1 Introduction

While the lattice calculations of hadron properties in the vacuum have reached quite satisfactory precision, little is known from such first principle calculations about basic hadronic parameters in a thermal medium, e.g. masses and widths at finite temperature. Lattice calculations of such quantities at zero temperature generally proceed through the calculation of correlation functions in Euclidean time. This approach naturally carries over to the calculation of spatial correlation functions at finite temperature. Such spatial correlation functions indeed show evidence for sudden changes of *in medium* hadron properties above T_c [1]. However, they provide only indirect evidence for modifications of, e.g. hadron masses and their widths. The appropriate approach here would be a detailed analysis of temporal correlation functions [2, 3], which at finite temperature are restricted to the Euclidean time interval $[0, 1/T]$. The interesting information on hadronic states is then encoded in the spectral functions for these correlators [4].

Currently available results from lattice calculations show significant changes in the behaviour of temporal correlation functions in the high temperature plasma phase of QCD [2, 3, 5, 6]. However, at least close to T_c the correlation functions clearly deviate from those of freely propagating quarks. It thus is important to understand in how far the temporal correlation functions carry information about the existence or non-existence of bound states or resonances in the plasma phase. Various calculations within the framework of low energy effective models also suggest strong modifications of hadron properties [7] and consequently also of the spectral functions [8]. However, it is difficult in such model calculations to deal with the quark substructure of hadrons, which will become important at high temperature where one expects to find indications for the propagation of almost free, massless quarks. Eventually it is the hope, that spectral methods [9], which successfully have been applied to hadron spectral functions at zero temperature [10], can also be applied at finite temperature. In particular, in the high temperature limit, well above the QCD phase transition temperature, it then might be appropriate to compare lattice calculations for temporal hadron correlators also with perturbative calculations. At least to some extend non-perturbative information can also be incorporated in such an analytic calculation by using the hard thermal loop (HTL) resummation scheme [11]. The recent successes in reproducing the QCD equation of state calculated on the lattice [12, 13] with HTL-resummed perturbative calculations for $T \gtrsim 2T_c$ [14, 15] suggest that this may be a reasonable starting point also for the description of other properties of the high temperature plasma phase [16]. Indeed, the spectral functions, which one will extract from an analysis of temporal correlators, are closely related to quark-antiquark annihilation processes in the quark-gluon plasma. For the vector channel this is linked to the dilepton production at high temperature, which has been studied in the HTL-approximation [17]. The temperature dependence of

the pseudo-scalar correlator is related to the chiral condensate. Thermal effects on this as well as the pseudo-scalar masses and dispersion relations influence the appearance or suppression of a disoriented chiral condensate which might lead to observable effects in relativistic heavy ion collisions [18].

We will analyze here the structure of temporal correlation functions at large temperature within the context of HTL-resummed perturbation theory. In the infinite temperature limit the free field behaviour is expected to give the dominant contribution to the correlation functions for energies $\omega \sim T$ [19, 20]. The HTL-resummed quark propagator [17, 21] goes beyond this leading order perturbative result and incorporates two non-perturbative features, which apparently will lead to competing effects in thermal correlation functions. On the one hand it takes into account the generation of thermal quark masses, $m_T \sim g(T)T$. This cuts off the low frequency part in the spectral functions and thus will lead to a steepening of thermal correlation functions. On the other hand it also contains the contributions from plasmino modes as well as interactions of quarks and antiquarks with gluons in the thermal heat bath (Landau damping). This enhances the contribution of soft modes with $\omega \sim g(T)T$ which, in fact, will dominate the structure of spectral functions at low energies even at rather high temperature [17]. These contributions from soft modes will lead to a flattening of thermal correlation functions. We will discuss the interplay between both features of HTL-resummed correlation functions in this paper.

In the next section we will present the framework for the calculation of thermal meson correlation functions in the HTL-approximation and give results for the scalar and vector spectral function. In Section 3 we compare the resulting thermal meson correlation functions with the leading order perturbative (free) correlators. Finally we give our conclusions in Section 4.

2 Thermal Meson Correlation Functions

2.1 Definitions

We want to analyze the behaviour of meson correlation functions in the high temperature limit. They are constructed from meson currents $J_M(\tau, \vec{x}) = \bar{q}(\tau, \vec{x})\Gamma_M q(\tau, \vec{x})$, where Γ_M is an appropriate combination of γ-matrices that fixes the quantum numbers of a meson channel; *i.e.,* $\Gamma_M = 1,\ \gamma_5,\ \gamma_\mu,\ \gamma_\mu\gamma_5$ for scalar, pseudo-scalar, vector and pseudo-vector channels, respectively. The thermal two-point functions in coordinate space, $G_M(\tau, \vec{x})$, are defined as

$$G_M(\tau, \vec{x}) \quad = \quad \langle J_M(\tau, \vec{x}) J_M^\dagger(0, \vec{0}) \rangle$$

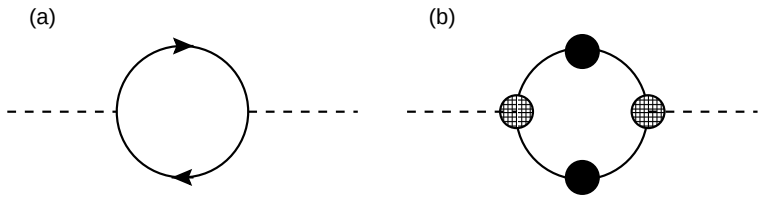

Figure 1: The self-energy diagrams for free quarks (a) and in the HTL approximation (b).

$$= \quad T \sum_{n=-\infty}^{\infty} \int \frac{\mathrm{d}^3 p}{(2\pi)^3} \, \mathrm{e}^{-i(\omega_n \tau - \vec{p}\vec{x})} \, \chi_M(\omega_n, \vec{p}) \quad , \tag{2.1}$$

where $\tau \in [0, 1/T]$, and the Fourier transformed correlation function $\chi_M(\omega_n, \vec{p})$ is given at the discrete Matsubara modes, $\omega_n = 2n\pi T$. The imaginary part of the momentum space correlator gives the spectral function $\sigma_M(\omega, \vec{p})$,

$$\chi_M(\omega_n, \vec{p}) = -\int_{-\infty}^{\infty} \mathrm{d}\omega \, \frac{\sigma_M(\omega, \vec{p})}{i\omega_n - \omega + i\epsilon} \quad \Rightarrow \quad \sigma_M(\omega, \vec{p}) = \frac{1}{\pi} \mathrm{Im} \, \chi_M(\omega, \vec{p}) \quad . \tag{2.2}$$

Using eqs. 2.1 and 2.2 we obtain the spectral representation of the thermal correlation functions in coordinate space at fixed momentum ($\beta = 1/T$),

$$G_M(\tau, \vec{p}) = \int_0^{\infty} \mathrm{d}\omega \, \sigma_M(\omega, \vec{p}) \, \frac{\cosh(\omega(\tau - \beta/2))}{\sinh(\omega\beta/2)} \quad . \tag{2.3}$$

For a perturbative analysis of these correlation functions at high temperature it is convenient to introduce dimensionless variables, $\tilde{\omega} = \omega/T$, $\vec{\tilde{p}} = \vec{p}/T$, $\tilde{\tau} = \tau T$ and the reduced spectral function $\tilde{\sigma}(\tilde{\omega}, \vec{\tilde{p}}) \equiv \sigma(\omega, \vec{p})/T^2$. In terms of these variables we find

$$\tilde{G}_M(\tilde{\tau}, \vec{\tilde{p}}) \equiv \frac{G_M(\tau, \vec{p})}{T^3} = \int_0^{\infty} \mathrm{d}\tilde{\omega} \, \tilde{\sigma}_M(\tilde{\omega}, \vec{\tilde{p}}) \, \frac{\cosh(\tilde{\omega}(\tilde{\tau} - 1/2))}{\sinh(\tilde{\omega}/2)} \quad . \tag{2.4}$$

2.2 Free Meson Spectral Functions

The starting point for a calculation of the meson spectral functions and the meson correlation functions is the momentum space representation of the latter [20]. To leading order perturbation theory one has to evaluate the self-energy diagram shown in Fig. 1a, where the internal quark lines represent a bare quark propagator

$S_F(k_0,\vec{k})$ which can be expressed in terms of its spectral function $\rho_F(\omega,\vec{k},m)$ and is conveniently written as

$$S_F(k_0,\vec{k}) = -(\gamma_0\ k_0 - \vec{\gamma}\cdot\vec{k} + m)\ \int_0^{1/T}\ \mathrm{d}\tau \mathrm{e}^{k_0\tau} \int_{-\infty}^{\infty}\ \mathrm{d}\omega \rho_F(\omega,\vec{k},m)\ [1-n_F(\omega)]\ \mathrm{e}^{-\omega\tau}, \quad (2.5)$$

where $k_0 = (2n+1)i\pi T$, $n_F(\omega) = 1/(1+\exp(\omega/T))$ and

$$\rho_F(\omega,\vec{k},m) = \frac{1}{2\omega}\ (\delta(\omega-\omega_k) + \delta(\omega+\omega_k)) \quad , \quad (2.6)$$

with $\omega_k = \sqrt{\vec{k}^2+m^2}$.

The thermal meson spectral functions are then obtained from eq. 2.2, that is from the imaginary part of the correlation functions in momentum space,

$$\chi_M(\omega,\vec{p}) = 2N_c T \sum_n \int \frac{\mathrm{d}^3k}{(2\pi)^3}\ \mathrm{Tr}\Big[\Gamma_M S_F(k_0,\vec{k})\Gamma_M^\dagger S_F^\dagger(\omega-k_0,\vec{p}-\vec{k})\Big] \quad (2.7)$$

In the case of free fermions this is easily evaluated. In the limit of vanishing external momentum one finds for the spectral functions,

$$\begin{aligned}\sigma_{\mathrm{M}}^{\mathrm{free}}(\omega,\vec{p}=0) \quad &= \quad \frac{N_c}{4\pi^2}\ \Theta(\omega-2m)\ \omega^2\ \tanh(\omega/4T)\ \sqrt{1-\left(\frac{2m}{\omega}\right)^2} \\ &\quad \cdot\left(a_M + \left(\frac{2m}{\omega}\right)^2 b_M\right) \quad , \end{aligned} \quad (2.8)$$

where different quantum number channels are characterized by the pair of parameters (a_M, b_M). For the scalar (s), pseudo-scalar (ps), vector (v) and pseudo-vector (pv) channels they are given by (-1,1), (1,0), (2,1) and (-2,3), respectively[b]. In the massless limit the spectral functions are chirally symmetric, $|\sigma_{ps}| = |\sigma_s|$ and $|\sigma_{pv}| = |\sigma_p|$. In this case the remaining integral in eq. 2.4 can be done analytically and one obtains for example in the pseudo-scalar case [20],

$$\tilde{G}_{ps}(\tilde{\tau},\vec{p}=0) = 2\pi N_c\ (1-2\tilde{\tau})\frac{1+\cos^2(2\pi\tilde{\tau})}{\sin^3(2\pi\tilde{\tau})} + 4N_c\ \frac{\cos(2\pi\tilde{\tau})}{\sin^2(2\pi\tilde{\tau})} \quad . \quad (2.9)$$

[b] In the vector and pseudo-vector cases we denote by σ_M the trace over the Lorentz indices of $\sigma_M^{\mu\nu}$.

2.3 HTL-Approximation for Meson Spectral Functions

Since in eq. 2.4 one has to integrate over soft ($\omega \simeq gT$) as well as hard ($\omega \sim T$) modes, a consistent computation of the temporal correlation functions at $\vec{p} = 0$ requires at least the use of HTL resummed propagators and vertices as shown in Fig. 1b [17]. In this way important medium effects of the quark-gluon plasma such as effective quark masses and Landau damping are taking into account. The above analysis for the free thermal meson correlators can then be extended to the leading order HTL approximation. The HTL-resummed fermion propagator is obtained from eq. 2.5 by replacing the free spectral function ρ_F with the HTL-resummed spectral function which for massless quarks is given by [17, 21]

$$\rho_{\rm HTL}(k_0, \vec{k}) = \frac{1}{2}\rho_+(k_0,k)(\gamma_0 - i\,\hat{k}\cdot\vec{\gamma}) + \frac{1}{2}\rho_-(k_0,k)(\gamma_0 + i\,\hat{k}\cdot\vec{\gamma}) \tag{2.10}$$

with $\hat{k} = \vec{k}/k$, $k = |\vec{k}|$, and

$$\begin{aligned}
\rho_\pm(k_0,k) &= \frac{k_0^2 - k^2}{2m_T^2}[\delta(k_0 - \omega_\pm) + \delta(k_0 + \omega_\mp)] + \beta_\pm(k_0,k)\Theta(k^2 - k_0^2) \qquad (2.11)\\
\beta_\pm(k_0,k) &= -\frac{m_T^2}{2}\frac{\pm k_0 - k}{\left[k(-k_0 \pm k) + m_T^2\left(\pm 1 - \frac{\pm k_0 - k}{2k}\ln\frac{k+k_0}{k-k_0}\right)\right]^2 + \left[\frac{\pi}{2}m_T^2\frac{\pm k_0 - k}{k}\right]^2}
\end{aligned}$$

Here $\omega_\pm(k)$ denote the two dispersion relations of quarks in a thermal medium [17, 21] and $m_T = g(T)T/\sqrt{6}$ is the thermal quark mass. We note that in addition to the appearance of two branches in the thermal quark dispersion relation the HTL-resummed fermion propagator also receives a cut-contribution below the light-cone ($k_0^2 < k^2$), which results from interactions of the valence quarks with gluons in the thermal medium (Landau damping). Furthermore, an explicit temperature dependence only enters through $m_T(T)$. Also the HTL-resummed quark spectral function can thus be written in terms of dimensionless, rescaled variables, e.g. $\tilde{\omega} = \omega/T$ etc. and the reduced meson spectral functions $\tilde{\sigma}^{\rm HTL} = \sigma^{\rm HTL}/T^2$ will depend on temperature only through $\tilde{m}_T = g(T)/\sqrt{6}$. It also should be noted that the HTL resummed quark propagator is chiral symmetric in spite of the appearance of an effective quark mass [21]. In the following we thus will ignore the parity of the meson states and will generically talk about scalar and vector channels only[c].

Inserting eq. 2.5 for $m = 0$ together with eq. 2.10 and eq. 2.11 into eq. 2.7 we can determine the spectral functions for mesons in the HTL-approximation. In the vector channel this also requires additional modifications of the vertex functions

[c] We will, however, show results for pseudo-scalar and vector spectral functions and correlators which in our notation are strictly positive.

Γ_M, *i.e.,* the use of a HTL quark-meson vertex, as discussed in detail in [17]. In the case of the scalar and pseudo-scalar spectral function the vertices are given by the bare vertices $\Gamma_s = 1$ and $\Gamma_{ps} = \gamma_5$, since contributions from a HTL resummation to the vertices are suppressed in this case, *i.e.* lead to higher order corrections, as discussed in the Yukawa theory [22] and scalar QED [23]. If, on the other hand, the bare vertex is proportional to γ_μ as in the vector meson case, the HTL vertex cannot be neglected, since in a gauge theory it is related to the HTL fermion propagator by Ward identities [24].

The pseudo-scalar spectral function can then be written as

$$\begin{aligned}\sigma_{\rm ps}(\omega,\vec{p}) &= 2N_c(\mathrm{e}^{\omega/T}-1)\int\frac{\mathrm{d}^3k}{(2\pi)^3}\int_{-\infty}^{\infty}\mathrm{d}x\mathrm{d}x'\; n_F(x)n_F(x')\delta(\omega-x-x') \\ &\cdot\Big\{(1-\vec{q}\cdot\vec{k})[\rho_+(x,k)\rho_+(x',q)+\rho_-(x,k)\rho_-(x,q)] \\ &+(1+\vec{q}\cdot\vec{k})[\rho_+(x,k)\rho_-(x',q)+\rho_-(x,k)\rho_+(x,q)]\Big\}, \qquad (2.12)\end{aligned}$$

where $\vec{q}=\vec{p}-\vec{k}$. The corresponding relation for the vector spectral function, which also includes HTL-vertex contributions, is related to the dilepton production rate calculated in Ref. [17] in the HTL approximation,

$$\sigma_{\rm v}(\omega,\vec{p}=0)=\frac{18\pi^2N_c}{5\alpha^2}\left(\mathrm{e}^{\omega/T}-1\right)\omega^2\frac{\mathrm{d}W}{\mathrm{d}\omega\mathrm{d}^3p}(\vec{p}=0)\;. \qquad (2.13)$$

Here α is the electromagnetic fine structure constant.

As the thermal meson correlation functions are constructed from two quark propagators, they will receive pole-pole, pole-cut and cut-cut contributions, *i.e.,* the mesonic spectral functions for $\vec{p}=0$ are generically given by

$$\sigma^{\rm HTL}(\omega)=\sigma^{\rm pp}(\omega)+\sigma^{\rm pc}(\omega)+\sigma^{\rm cc}(\omega)\quad. \qquad (2.14)$$

Explicit expressions for the three different contributions to the pseudo-scalar spectral function, $\sigma_{\rm ps}^{\rm HTL}$, are given in the Appendix. Similar results for the vector spectral function $\sigma_{\rm v}^{\rm HTL}$ have been derived in [17] where also a detailed discussion of the physical processes related to the pole-pole, pole-cut and cut-cut contributions is given. In particular, there are characteristic peaks that show up in the pole-pole contribution (van Hove singularities). They are caused by a diverging density of states which is inversely proportional to the derivative of the dispersion relations, $\omega'_\pm(k)$, appearing in eq. A.1. Owing to the minimum in the plasmino branch[d] these

[d] In Ref.[25] it has been argued that the full in-medium quark propagator leads in general to two branches in the dispersion relation, of which one exhibits a minimum.

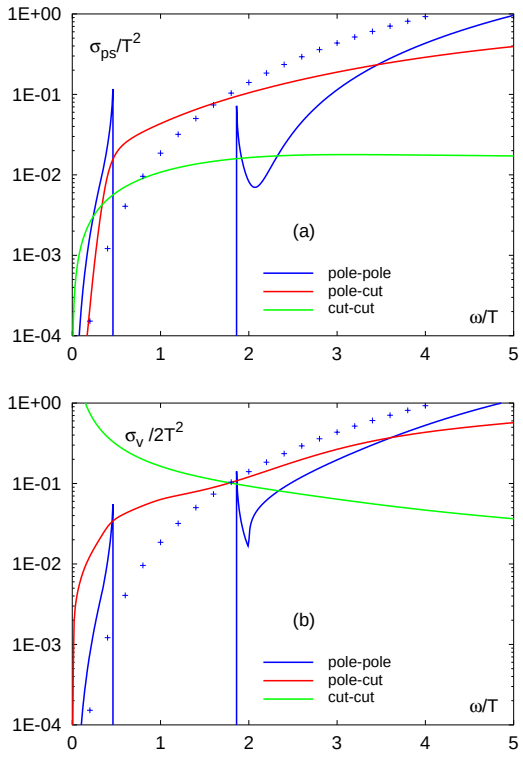

Figure 2: The pole-pole, pole-cut and cut-cut contributions to the pseudo-scalar (a) and vector (b) spectral function for $\tilde{m}_T = 1$. The crosses show the free meson spectral function.

derivatives vanish at $\omega = 0.47 m_T$ and $1.856 m_T$. Apart from values close to the van Hove singularities in $\sigma^{\rm pp}$ one finds that the cut contributions dominate the spectral function for small values of $\tilde{\omega}$, e.g. for $\tilde{\omega} \lesssim g(T)$.

In Fig. 2 we show the pole ($\tilde{\sigma}^{\rm pp}$) and cut ($\tilde{\sigma}^{\rm pc}$, $\tilde{\sigma}^{\rm cc}$) contributions to the scalar (Fig. 2a) and vector (Fig. 2b) spectral functions for the case $\tilde{m}_T = 1$, extrapolating the HTL results, obtained in the weak coupling limit, to $g = \sqrt{6}$. As can be seen in Fig. 2 the pole and cut contributions influence the spectral function in different ways. The former gives the dominant contribution for large $\tilde{\omega}$. The deviations of $\sigma^{\rm HTL}$ from the free spectral function in this energy regime as well as the threshold for $\tilde{\omega} \simeq 2\ \tilde{m}_T$ is due to the presence of a non-vanishing thermal mass in the quark dispersion relation and reflects the almost free propagation of two quarks in the plasma. Additional interactions of these quarks with the thermal medium (Landau damping) are represented by the cut contributions. These lead to an enhancement over the free spectral functions for small values of $\tilde{\omega}$ as discussed above. Furthermore, we note that the pole-pole and pole-cut contributions to the spectral functions are similar in the scalar and vector channels. The cut-cut contribution, however,

behaves differently at small energies. While it vanishes for small $\tilde{\omega}$ in the scalar channel it diverges linearly in the vector channel. This can be traced back to the structure of the effective HTL-vertex, which contains a collinear singularity [26]. As a consequence of this singularity infinitely many higher order diagrams in the HTL expansion contribute to the same order in the coupling constant [27]. This, of course, indicates that the low frequency part of the vector spectral functions is inherently non-perturbative.

3 HTL-Approximation for Thermal Meson Correlators

3.1 Thermal Pseudo-Scalar Meson Correlation Function

The competing influence of pole and cut contributions to the HTL-resummed spectral functions carries over to the behaviour of thermal meson correlation functions. The appearance of a non-vanishing thermal quark mass tends to lead to a more rapid decrease of the correlator in Euclidean time than this is the case for the free massless correlator. The enhancement of the low energy part which is due to the cut contributions, on the other hand, will counteract this trend. This is evident from the behaviour of thermal meson correlation functions in the scalar channel which is shown in Fig. 3 for $\tilde{m}_T = 1$ and 2. As expected the correlator constructed from the pole-pole contribution alone is steeper than the free correlator and, moreover, is strongly dependent on $\tilde{m}_T$. The cut contributions, however, enhance the low energy contributions in the spectral function and thus flattens the correlator again. Somewhat surprisingly for $\tilde{m}_T \simeq 1$ this seems to compensate almost completely the deviations from the free correlator introduced by the pole contributions. The difference between the free and HTL-resummed correlators is largest for $\tau T \simeq 1/2$ where the contribution from the low energy regime in the spectral function is largest. For $\tau T \to 0$, and $\tau T \to 1$, on the other hand, the free and HTL-resummed correlators approach each other as $\lim_{\omega\to\infty} \sigma^{\rm HTL}(\omega)/\sigma^{\rm free}(\omega) = 1$. These features are amplified in the ratio $G_{ps}^{\rm HTL}(\tau)/G_{ps}^{\rm free}(\tau)$ which is shown in Fig. 4.

3.2 Thermal Vector Meson Correlation Function

As already discussed in section 2.1 the calculation of the vector correlators within the HTL method requires the use of effective quark-meson vertices as shown in Fig. 1b. This does lead to a linear divergence of the spectral function in the vector channel at low frequencies, which in turn renders the temporal correlator infrared divergent. In fact, although the scalar correlation functions are infrared finite, it is

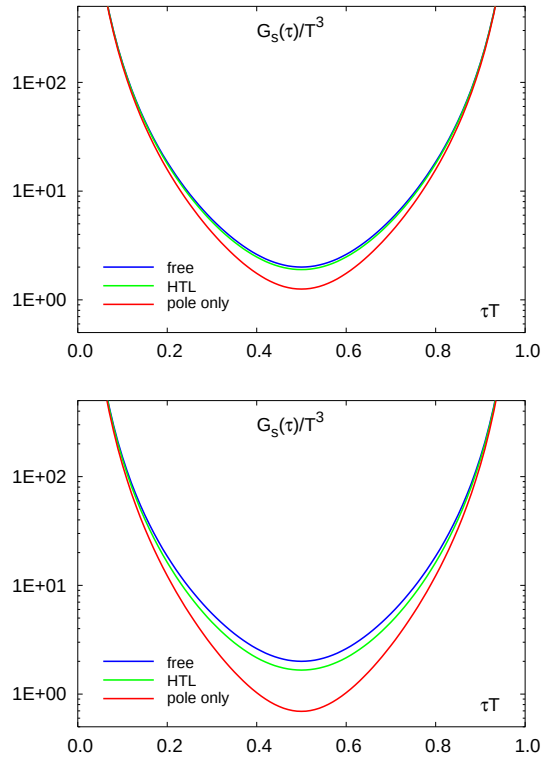

Figure 3: The thermal pseudo-scalar meson correlation function in the HTL approximation for $\tilde{m}_T = 1$ (left) and $\tilde{m}_T = 2$ (right). The curves shown the complete thermal correlator (middle line), the correlator constructed from σ_s^{pp} only (lower line) and the free thermal correlator (upper line).

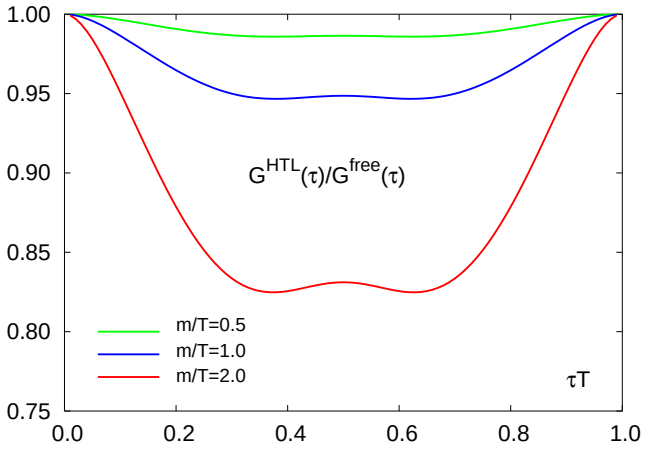

Figure 4: The ratio of the HTL-resummed and free thermal pseudo-scalar correlation function versus Euclidean time τ in units of the temperature. Shown are results for thermal quark masses $\tilde{m}_T = 0.5$ (top), 1.0 (middle) and 2.0 (bottom).

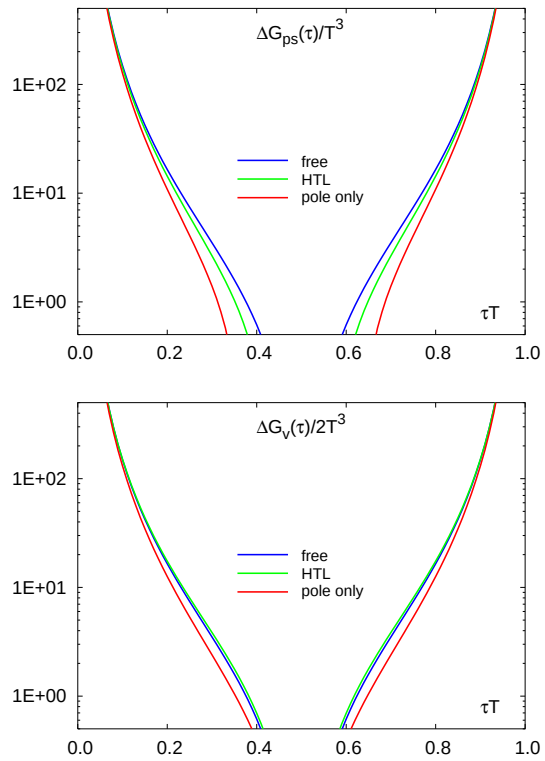

Figure 5: The subtracted thermal pseudo-scalar (left) and vector (right) meson correlation functions in the HTL approximation for $\tilde{m}_T = 2$. The curves shown the complete thermal correlator (middle line), the correlator constructed from $\sigma_{\rm ps}^{\rm pp}$ only (lower line) and the free thermal correlator (upper line).

to be expected, that also in this case the low frequency part of the HTL-resummed spectral functions will be modified significantly from contributions of higher order diagrams. It thus seems to be reasonable to consider modified correlation functions, which are less sensitive to details of the low frequency part of the spectral functions. We therefore define the subtracted correlators

$$\Delta\tilde{G}_M(\tau) \equiv \tilde{G}_M(\tau) - \tilde{G}_M(\beta/2) \ . \tag{3.1}$$

In the subtracted correlation functions the infrared divergences are eliminated. They are well-defined in the scalar as well as in the vector channels. In Fig. 5 we compare the HTL-resummed subtracted correlation functions with corresponding results for the free case. This shows that after elimination of the infrared divergent parts the structure of the pole and cut contributions is similar in scalar and vector channels. The vector correlator seems to be even closer to the leading order perturbative (free) correlator than the scalar correlation function.

4 Conclusions

We have calculated thermal meson correlation functions and their spectral functions in the HTL-approximation. We have analyzed the influence of the various contributions to the HTL-resummed scalar and vector meson spectral functions on the structure of the thermal correlators. We generally find that the correlators in HTL-approximation – after subtracting the infrared singularity in the vector correlator – are quite similar to those calculated in leading order perturbation theory which correspond to free correlation functions. Non-perturbative features of the HTL-resummed quark propagators such as the generation of a thermal quark mass and Landau damping are clearly visible in the meson spectral functions. However, they lead to competing effects in the correlation functions and to a large extent compensate each other.

The main difference between the scalar and the vector channel using the HTL approximation is the different behaviour of the cut-cut contribution to the spectral functions at small energies. The vector spectral function diverges in the infrared limit leading to a singular expression for the vector correlation function. This feature is in agreement with the observation, that the dilepton production rate, which is closely related to the vector spectral function, cannot be computed within the HTL improved perturbation scheme for small invariant masses $M \simeq g^2 T$.

The existing lattice calculations of thermal meson correlation functions show that the correlators deviate from the free field result significantly for temperatures $T \lesssim 2T_c$. However, also at larger temperatures it seems that the scalar correlator only slowly approaches the free correlation function and still differs in shape from the vector correlator. This suggests that HTL-resummed perturbation theory, which gave a satisfactory description of bulk thermodynamics above $2T_c$, will not be appropriate for a quantitative analysis of thermal meson correlation functions at least in the pseudo-scalar case. In other words, the HTL medium effects (thermal quark masses, Landau damping) are not sufficient to explain the deviations of the pseudo-scalar correlator from the free one as observed in lattice calculations. Therefore additional non-perturbative effects, maybe related to chiral symmetry restoration, appear to be important in the pseudo-scalar channel.

Acknowledgements:

The work of FK has been supported by the TMR network ERBFMRX-CT-970122 and the DFG under grant Ka 1198/4-1. MGM would like to acknowledge support from AvH Foundation as part of this work was initiated during his stay at the University of Giessen as an Humboldt Fellow.

Appendix

We will give here explicit expressions for the pole-pole, pole-cut and cut-cut contributions to the pseudo-scalar spectral function. The pole-pole contribution ($\vec{p}=0$) is given by

$$\begin{aligned}\sigma_{\rm ps}^{\rm pp}(\omega) &= \frac{N_c}{2\pi^2} m_T^{-4}(\mathrm{e}^{\omega/T}-1)\Big[n_F^2(\omega_+(k_1))(\omega_+^2(k_1)-k_1^2)^2\frac{k_1^2}{2|\omega_+'(k_1)|} \\ &+ 2\sum_{i=1}^{2} n_F(\omega_+(k_2^i))[1-n_F(\omega_-(k_2^i))](\omega_-^2(k_2^i)-(k_2^i)^2)(\omega_+^2(k_2^i)-(k_2^i)^2)\cdot \\ &\qquad \cdot\frac{(k_2^i)^2}{|\omega_+'(k_2^i)-\omega_-'(k_2^i)|} \\ &+ \sum_{i=1}^{2} n_F^2(\omega_-(k_3^i))(\omega_-^2(k_3^i)-(k_3^i)^2)^2\frac{(k_3^i)^2}{2|\omega_-'(k_3^i)|}\Big] \quad . \end{aligned} \tag{A.1}$$

Here $\omega_\pm(k)$ denote the quark dispersion relations for the ordinary quark (+) and the plasmino (-) branch [17], k_1 is the solution of $\omega-2\omega_+(k_1)=0$, k_2^i and k_3^i are the solutions of $\omega-\omega_+(k_2^i)+\omega_-(k_2^i)=0$ and $\omega-2\omega_-(k_3^i)=0$, respectively. Note that for small momenta the last two equations can each have two solutions. Furthermore, $\omega_\pm'(k)\equiv(\mathrm{d}\omega_\pm(x)/\mathrm{d}x)|_{x=k}$. For the pole-cut contribution we find

$$\begin{aligned}\sigma_{\rm ps}^{\rm pc}(\omega) &= \frac{2N_c}{\pi^2} m_T^{-2}(\mathrm{e}^{\omega/T}-1)\int_0^\infty \mathrm{d}k\; k^2\cdot \\ &\cdot \Big[\;\Theta(k^2-(\omega-\omega_+)^2)n_F(\omega-\omega_+)n_F(\omega_+)\beta_+(\omega-\omega_+,k)(\omega_+^2-k^2) \\ &\quad +\Theta(k^2-(\omega-\omega_-)^2)n_F(\omega-\omega_-)n_F(\omega_-)\beta_-(\omega-\omega_-,k)(\omega_-^2-k^2) \\ &\quad +\Theta(k^2-(\omega+\omega_-)^2)n_F(\omega+\omega_-)[1-n_F(\omega_-)]\beta_+(\omega+\omega_-,k)(\omega_-^2-k^2) \\ &\quad +\Theta(k^2-(\omega+\omega_+)^2)n_F(\omega+\omega_+)[1-n_F(\omega_+)]\beta_+(\omega+\omega_+,k)(\omega_+^2-k^2)\Big]\end{aligned} \tag{A.2}$$

Finally we obtain for the cut-cut contribution

$$\begin{aligned}\sigma_{\rm ps}^{\rm cc}(\omega) &= \frac{2N_c}{\pi^2}(\mathrm{e}^{\omega/T}-1)\int_0^\infty \mathrm{d}k\; k^2\int_{-k}^{k}\mathrm{d}x\; n_F(x)n_F(x-\omega)\Theta(k^2-(x-\omega)^2)\cdot \\ &\qquad \cdot\Big[\beta_+(x,k)\beta_+(\omega-x,k)+\beta_-(x,k)\beta_-(\omega-x,k)\Big]\end{aligned} \tag{A.3}$$

The resulting contributions to the thermal correlator are then given by eq. 2.3.

References

[1] C. DeTar and J.B. Kogut, Phys. Rev. D36 (1987) 2828.

[2] T. Hashimoto, A. Nakamura and I.O. Stamatescu, Nucl. Phys. B400 (1993) 267.

[3] G. Boyd, S. Gupta, F. Karsch and E. Laermann, Z. Phys. C 64 (1994) 331.

[4] for a review see: E.V. Shuryak, Rev. Mod. Phys. 65 (1993) 1.

[5] S. Gupta, F. Karsch, E. Laermann, B. Petersson and K. Redlich, Phys. Lett. B349 (1995) 170.

[6] Ph. de Forcrand et al. (QCDTARO collaboration), Mesons above the deconfining transition, hep-lat/9901017.

[7] G.E. Brown and M. Rho, Phys. Rev. Lett. 66 (1991) 2720; B. Friman and H.J. Pirner, Nucl. Phys. A 617 (1997) 496; R. Rapp, G. Chanfray, and J. Wambach, Nucl. Phys. A 617 (1997) 472; F. Klingl, N. Kaiser, and W. Weise, Nucl. Phys. A 624 (1997) 527; W. Peters, M. Post, H. Lenske, S. Leupold, and U. Mosel, Nucl. Phys. A 632 (1998) 109; W. Cassing, E.L. Bratkovskaya, R. Rapp, and J. Wambach, Phys. Rev. C 57 (1998) 916; M.H. Thoma, S. Leupold, and U. Mosel, Eur. Phys. J. A7 (2000) 219.

[8] S. Chiku and T. Hatsuda Phys. Rev. D58 (1998) 076001.

[9] for a review see: M. Jarrell and J.E. Gubernatis, Phys. Rep. 269 (1996) 133.

[10] Y. Nakahara, M. Asakawa and T. Hatsuda, Phys. Rev. D60 (1999) 091503.

[11] E. Braaten and R.D. Pisarski, Nucl. Phys. B 337 (1990) 569.

[12] G. Boyd, J. Engels, F. Karsch, E. Laermann, C. Legeland, M. Lütgemeier and B. Petersson, Phys. Rev. Let. 75 (1995) 4169 and Nucl. Phys. B469 (1996) 419.

[13] F. Karsch, E. Laermann and A. Peikert, Phys. Lett. B478 (2000) 447.

[14] J.-P. Blaizot, E. Iancu and A. Rebhan, Phys. Rev. Lett. 83 (1999) 2906; Phys. Lett. B 470 (1999) 181; hep-ph/0005003.

[15] J.O. Andersen, E. Braaten and M. Strickland, Phys. Rev. Lett. 83 (1999) 2139; Phys. Rev. D 61 (2000) 014017, 074016.

[16] M.H. Thoma, Nucl. Phys. A 638 (1998) 317c.

[17] E. Braaten, R.D. Pisarski and T. C. Yuan, Phys. Rev. Lett. 64 (1990) 2242.

[18] See e.g. J. Schaffner-Bielich and J. Randrup, Phys. Rev. C59 (1999) 3329.

[19] V.L. Eletskii and B.L. Yoffe, Sov. J. Nucl. Phys. 48 (1988) 384.

[20] W. Florkowski and B.L. Friman, Z. Phys. A347 (1994) 271.

[21] V.V. Klimov, Sov. Phys. JETP 55 (1982) 199;
H.A. Weldon, Phys. Rev. D 26 (1982) 2789.

[22] M.H. Thoma, Z. Phys. C 66 (1995) 491.

[23] U. Kraemmer, A.K. Rebhan, and H. Schulz, Ann. Phys. (N.Y.) 238 (1995) 286.

[24] E. Braaten and R.D. Pisarski, Nucl. Phys. B 339 (1990) 310.

[25] A. Peshier and M.H. Thoma, Phys. Rev. Lett. 84 (2000) 841.

[26] R. Baier, S. Peigné and D. Schiff, Z. Phys. C 62 (1994) 337.

[27] P. Aurenche, F. Gelis, R. Kobes and H. Zaraket, Phys. Rev. D 58 (1998) 085003;
P. Aurenche, F. Gelis and H. Zaraket, Phys. Rev. D 61 (2000) 116001.